Supporting Information

of

Analysis of heat and mass transfer limitations for the combustion of methane emissions on PdO/Co_3O_4 coated on ceramic open cell foams

Carmen W. Moncada Quintero[1], Giuliana Ercolino[1], Abhinav Poozhikunnath[2,3], Radenka Maric[2,3], Stefania Specchia[1]**

[1] *Politecnico di Torino, Department of Applied Science and Technology, Corso Duca degli Abruzzi 24, 10129 Torino, Italy*

[2] *University of Connecticut, Department of Materials Science and Engineering, 97 North Eagleville Road, Storrs, CT 06269, USA*

[3] *University of Connecticut, Center for Clean Energy Engineering, 44 Weaver Road, Storrs, CT, 06269-5233, USA*

* Corresponding authors: carmen.moncada@polito.it, stefania.specchia@polito.it

In the following, a detailed explanation of the calculations of textural and geometrical properties of the OCF and the characteristic length scales for transverse diffusion is reported.

S.1. Estimation of the textural and geometrical properties of the OCF

The volume of the OCF was calculated as:

$$V_{OCF} = \frac{\pi \cdot d_{OCF}^2}{4} \cdot L_{OCF} \quad \text{A.1}$$

where V_{OCF} is the volume of the OCF (m^3), d_{OCF} is the diameter of the OCF ($d_{OCF} = 9 \cdot 10^{-3}\ m$) and L_{OCF} is the length of the OCF ($L_{OCF} = 30 \cdot 10^{-3}\ m$).

The face diameter of the OCF was determined by [1]:

$$d_f = d_p + t_s \quad \text{A.2}$$

where d_f is the face diameter of the OCF (m), d_p is the average pore diameter of the OCF (measured by SEM : Zir-OCF = 1.30 ± 0.73 mm; Alu-OCF = 1.34 ± 0.55 mm and SiC-OCF = 1.63 ± 0.65 mm) and t_s is the average strut thickness of the OCF (measured by SEM: Zir-OCF = 0.47 ± 0.16 mm; Alu-OCF = 0.34 ± 0.10 mm and SiC-OCF = 0.42 ± 0.16 mm) [2]

The foam relative density of the OCF was calculated by:

$$\rho_r = 2.59 \cdot \left(\frac{t_s}{d_f}\right)^2 \quad \text{A.3}$$

where t_s is the average strut thickness of the OCF and d_f is the face diameter of the OCF (m).

The voidage of the OCF was determined as:

$$\varepsilon = 1 - \rho_r \quad \text{A.4}$$

where ε is the voidage of the OCF (-).

The geometrical surface area of the OCF was calculated as:

$$S_{ga} = \frac{4.82}{d_f} \cdot \sqrt{\rho_r} \quad \text{A.5}$$

where S_{ga} is the geometrical surface area of the OCF (m^{-1}).

The surface area of the OCF was determined by:

$$S_a = V_{OCF} \cdot S_{ga} \quad \text{A.6}$$

where S_a is the surface area of the OCF (m^2).

The catalyst loading was calculated as:

$$C_{load} = \frac{m_{cat}}{S_a} \quad \text{A.7}$$

where C_{load} is the catalyst loading on the OCF (g m^{-2}) and m_{cat} is the catalyst mass deposited on the OCF (g).

The catalyst thickness on the OCF was calculated as:

$$\delta = \frac{C_{load}}{\rho_{cat}} \quad \text{A.8}$$

where δ is the catalyst thickness on the OCF (m) and ρ_{cat} is the catalyst density ($\rho_{cat} = 2 \cdot 10^6\ g \cdot m^3\ for\ 3\ wt.\%\ Pd/Co_3O_4$).

S.2. Estimation of the characteristic length scale for transverse diffusion

S.2.1 Characteristic length scale for the gas phase

The characteristic length scale for the gas phase ($R_{\Omega,e}$) is defined as the ratio of the flow area ($A_{\Omega,e}$) to the gas-coated layer interfacial perimeter (P_Ω).

Assuming that the Pd/Co_3O_4 catalyst is uniformly distributed inside the pores of the OCF and considering that the shape of both the pore and the catalytic layer is circular (**Fig. S3.1** Case A.), the $R_{\Omega,e}$ (m) was determined as [3–5]:

$$R_{\Omega,e} = \frac{A^c_{\Omega,e}}{P^c_\Omega} \quad \text{A.9}$$

$$A^c_{\Omega,e} = \frac{\pi \cdot d^2_{p_c}}{4} \quad \text{A.10}$$

$$P^c_\Omega = \pi \cdot d_{p_c} \quad \text{A.11}$$

where $A^c_{\Omega,e}$ is the cross-sectional area of fluid phase for circular shape of the pore and catalyst layer (m^2), d_{p_c} is the catalyst-coated pore diameter of the OCF (where $d_{p_c}(m) = 2 \cdot R_1$), P^c_Ω is the gas-coated catalyst layer circular interfacial perimeter (m).

Similarly, assuming oval shape of the pore and catalyst coated layer (**Fig. S3.2** Case B.), the $R_{\Omega,\mathrm{e}}$ (m) was determined considering the properties of an oval as:

$$R_{\Omega,\mathrm{e}} = \frac{A^{o}_{\Omega,\mathrm{e}}}{P^{o}_{\Omega}} \quad \text{A.12}$$

$$A^{o}_{\Omega,\mathrm{e}} = \pi \cdot a_f \cdot b_f \quad \text{A.13}$$

$$P^{o,*}_{\Omega} = 2 \cdot \pi \sqrt{\frac{{a_f}^2 + {b_f}^2}{2}}; \text{ for } b_f < 3 \cdot a_f \quad \text{A.14}$$

$$P^{o,**}_{\Omega} = \pi \cdot \left[3 \cdot \left(a_f + b_f\right) - \sqrt{(3 \cdot a_f + b_f) \cdot (a_f + 3 \cdot b_f)}\right] \quad \text{A.15}$$

where $A^{o}_{\Omega,\mathrm{e}}$ is the cross-sectional area of fluid phase for oval shape of the pore and catalyst layer (m^2), a_f is the semi-minor axe of the oval coated pore (m), b_f is the semi-major axe of the oval coated pore (m), $P^{o,*}_{\Omega}$ (m) is the gas-coated catalyst layer oval interfacial perimeter (Eq. A.14 valid when $b_f < 3 \cdot a_f$), $P^{o,**}_{\Omega}$ (m) is the gas-coated catalyst layer oval interfacial perimeter derived by Ramanujan.

To study the general situation in which the catalyst is deposited preferentially in some areas of the pore, accumulating a thicker layer of catalyst (δ_{max}), while in other zones of the pore only a thin catalytic layer is deposited (δ_{min}), we consider the case of an OCF with oval pore shape where the catalyst is deposited inside the inner wall of the pore with a circular shape of catalytic layer (**Fig. S3.3** Case C.). Thus, the $R_{\Omega,\mathrm{e}}$ (m) was calculated as:

$$R_{\Omega,\mathrm{e}} = \frac{A^{cc}_{\Omega,\mathrm{e}}}{P^{cc}_{\Omega}} \quad \text{A.16}$$

$$A^{oc}_{\Omega,\mathrm{e}} = \frac{\pi \cdot {d^2_p}_{cc}}{4} \quad \text{A.17}$$

$$P^{oc}_{\Omega} = \pi \cdot {d_p}_{cc} \quad \text{A.18}$$

where $A^{cc}_{\Omega,\mathrm{e}}$ is the cross-sectional area of fluid phase for circular shape of the catalyst layer (m^2), ${d_p}_{cc}$ is the catalyst-coated pore diameter of the OCF (m), P^{cc}_{Ω} (m) is the gas-coated catalyst layer circular interfacial perimeter (considering oval bare pore of OCF and circular coated layer shape).

S.2.2 Characteristic length scale for the coated layer

The characteristic length scale for the catalyst layer ($R_{\Omega,\mathrm{i}}$) is defined as the ratio of coated catalyst layer cross-sectional area ($A_{\Omega,\mathrm{i}}$) to the interfacial perimeter (P_{Ω}).

For the case A (pore and coated catalyst layer with circular shape), the $R_{\Omega,\mathrm{i}}$ (m) was determined as [3–5]:

$$R_{\Omega,\mathrm{i}} = \frac{A^{c}_{\Omega,\mathrm{i}}}{P^{c}_{\Omega}} \quad \text{A.19}$$

$$A^{c}_{\Omega,\mathrm{i}} = \frac{\pi}{4} \cdot ({d^2_p}_b - {d^2_p}_c) \quad \text{A. 20}$$

where $A^{c}_{\Omega,\mathrm{i}}$ is the cross-sectional area of the coated catalyst layer for circular shape of the bare pore and coated catalyst (m^2), d_{p_b} (m) is the pore diameter of the bare OCF (where $d_{p_b} = 2 \cdot R_2$).

For the case B (oval shape of the pore and coated catalyst layer), the $R_{\Omega,\mathrm{i}}$ (m) was determined as:

$$R_{\Omega,\mathrm{i}} = \frac{A^{o}_{\Omega,\mathrm{i}}}{P^{o}_{\Omega}} \quad \text{A.21}$$

$$A^{o}_{\Omega,\mathrm{i}} = \pi \cdot (a_{p,m} \cdot b_{p,m} - a_f \cdot b_f) \quad \text{A.22}$$

where $A^{o}_{\Omega,\mathrm{i}}$ is the cross-sectional area of the coated catalyst layer for oval shape of the bare pore and coated catalyst (m^2), $a_{p,m}$ is the average of semi-minor axe of the oval bare pore (m), $b_{p,m}$ is the average of semi-major axe of the oval coated pore (m), P^{o}_{Ω} (m) is the gas-coated catalyst layer oval interfacial perimeter (calculated using Equation A.14 or A.15)

For the case C (oval pore shape and circular shape of the coated catalyst layer), the $R_{\Omega,\mathrm{i}}$ (m) was calculated as:

$$R_{\Omega,\mathrm{i}} = \frac{A^{oc}_{\Omega,\mathrm{i}}}{P^{oc}_{\Omega}} \quad \text{A.23}$$

$$A^{oc}_{\Omega,\mathrm{i}} = \frac{\pi \cdot d^{2}_{poc}}{4} \quad \text{A.24}$$

where $A^{oc}_{\Omega,\mathrm{i}}$ is the cross-sectional area of the coated catalyst layer for oval shape of the bare pore and circular shape of the coated catalyst layer (m^2), $d_{p_{oc}}$ (m) is the catalyst-coated pore diameter (where $d_{p_{oc}} = 2 \cdot R_f$).

S.3. FESEM images

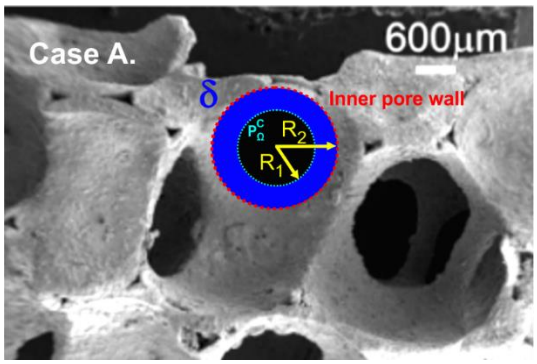

Fig. S3.1 SEM micrographs of Zir-OCF with 30 ppi considering case A: Circular shape of the pore and coated catalyst layer.

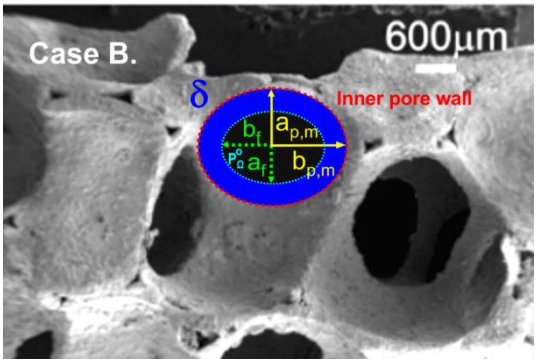

Fig. S3.2 SEM micrographs of Zir-OCF with 30 ppi considering case B: Oval shape of the pore and coated catalyst layer.

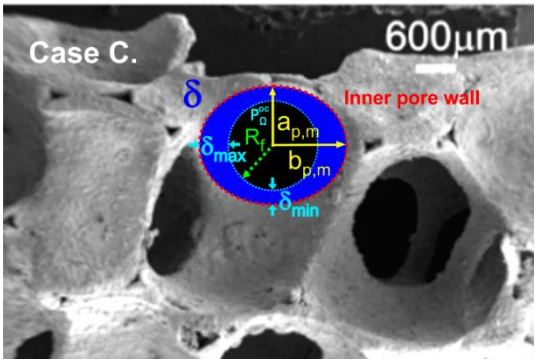

Fig. S3.3 SEM micrographs of Zir-OCF with 30 ppi considering case C: Oval shape of the pore and circular shape of the coated catalyst layer.

S.4. Diffusion and kinetic resistances of the cases A, B, and C.

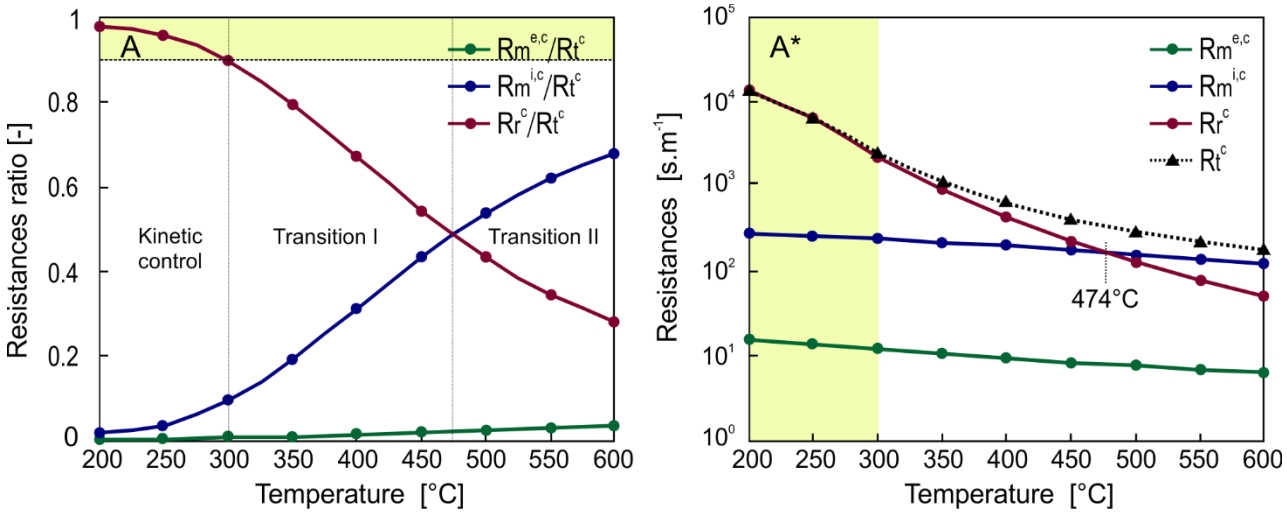

Fig. S4.1 Resistances ratio (A) and resistances (A*) as a function of temperature for the case A: Circular shape of the pore and coated catalyst layer.

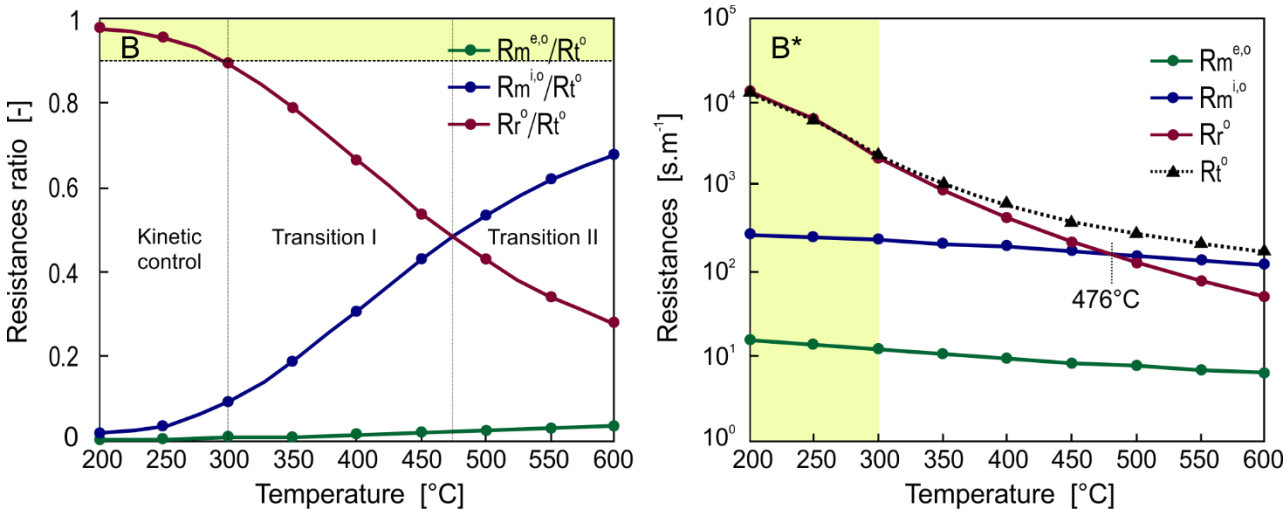

Fig. S4.2 Resistances ratio (B) and resistances (B*) as a function of temperature for the case B: Oval shape of the pore and coated catalyst layer.

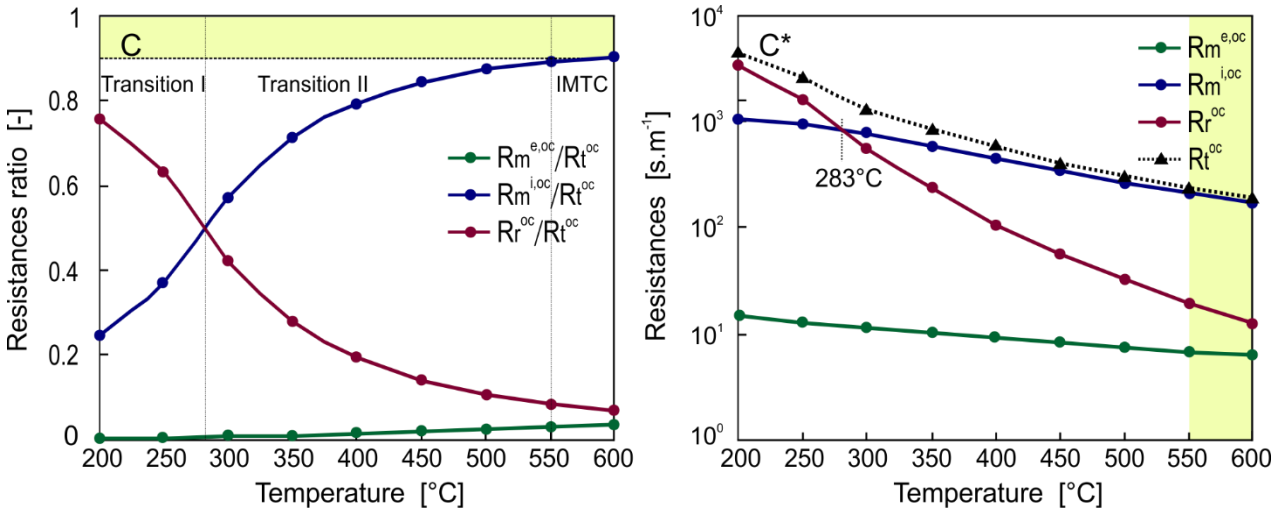

Fig. S4.3 Resistances ratio (C) and resistances (C*) as a function of temperature for the case C: Oval shape of the pore and circular shape of the coated catalyst layer.

S.4 Comparison of the effects of external and internal heat transfer of the cases A, B and C.

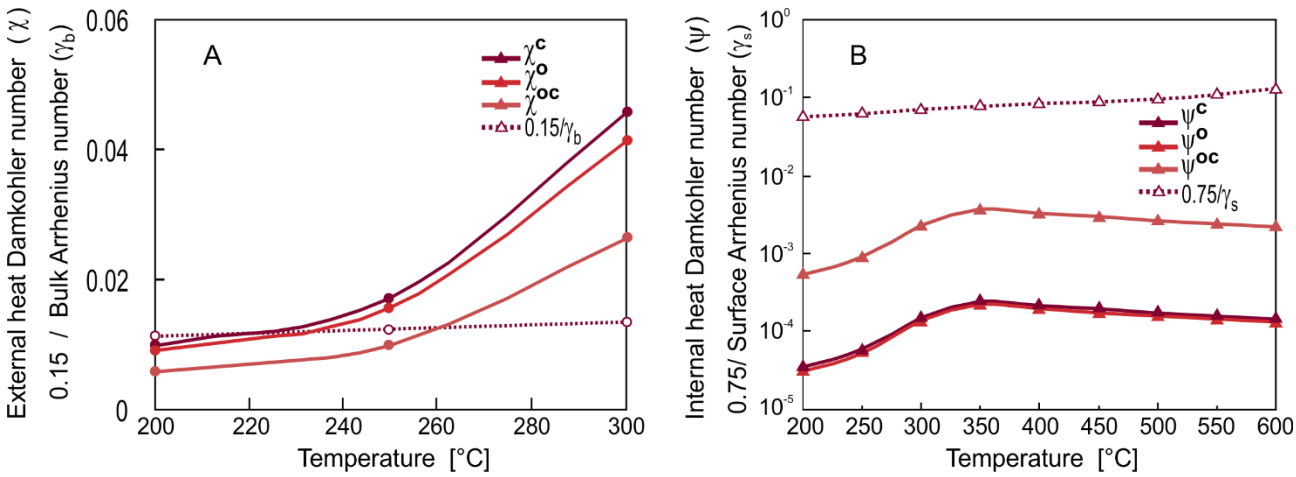

Fig. S.4.1 Criteria for evaluating the effects of external heat transfer (A) and internal heat transfer (B) for the case A, B and C.

References

[1] F.C. Buciuman, B. Kraushaar-Czarnetzki, Ceramic foam monoliths as catalyst carriers. 1. Adjustment and description of the morphology, Ind. Eng. Chem. Res. 42 (2003) 1863–1869. doi:10.1021/ie0204134.

[2] G. Ercolino, P. Stelmachowski, S. Specchia, Catalytic performance of Pd/Co_3O_4 on SiC and ZrO_2 open cell foams for process intensification of methane combustion in lean conditions, Ind. Eng. Chem. Res. 56 (2017) 6625–6636. doi:10.1021/acs.iecr.7b01087.

[3] S.Y. Joshi, M.P. Harold, V. Balakotaiah, On the use of internal mass transfer coefficients in modeling of diffusion and reaction in catalytic monoliths, Chem. Eng. Sci. 64 (2009) 4976–4991. doi:10.1016/j.ces.2009.08.008.

[4] S.Y. Joshi, M.P. Harold, V. Balakotaiah, Overall mass transfer coefficients and controlling regimes in catalytic monoliths, Chem. Eng. Sci. 65 (2010) 1729–1747. doi:10.1016/j.ces.2009.11.021.

[5] S.Y. Joshi, Y. Ren, M.P. Harold, V. Balakotaiah, Determination of kinetics and controlling regimes for H_2 oxidation on Pt/Al_2O_3 monolithic catalyst using high space velocity experiments, Appl. Catal. B Environ. 102 (2011) 484–495. doi:10.1016/j.apcatb.2010.12.030.